Desalination and Water Treatment
www.deswater.com

doi: 10.5004/dwt.2022.27952

245 (2022) 286–296
January

Removal of methylene blue from aqueous solution using a mixture of dried rice husk, sugarcane bagasse and wheat bran powder as a low-cost biosorbent

T. Malarvizhi[a,*], K. Muthukumaran[b], P. Thamarai[c]

[a]*Department of Industrial Biotechnology, Government College of Technology, Coimbatore, India, email: malarvizhit@gct.ac.in*
[b]*Department of Chemistry, Government College of Technology, Coimbatore, India, email: bamikumar@gct.ac.in*
[c]*Departmentof Environmental Engineering, Government College of Technology, Coimbatore, India, email: principal@gct.ac.in*

Received 15 July 2021; Accepted 29 October 2021

ABSTRACT

Dye removal from textile industrial wastewater through conventional methods is a critical task over the last few decades. This article focuses on an efficient and economic biosorption technique used to study the elimination of methylene blue (MB) from wastewater. A mixture of dried rice husk, sugarcane bagasse and wheat bran powder (DRSWP) in equal amounts was used to prepare a biosorbent to remove the methylene blue (MB) dye. This work discusses the impacts of different variables such as pH, contact time, initial dye concentration and biosorbent dose during the dye molecule elimination process and the optimal experimental conditions were also determined. As a result, the removal percentage of MB dye was found to be 96%. The equilibrium data were studied by Langmuir, Freundlich and Temkin isotherm models. The examined data suited well with the Langmuir model having a maximum biosorption capacity of 39.002 mg/g of DRSWP-biosorbent for MB. The pseudo-first-order kinetic equation effectively explained the kinetics of biosorption of MB using DRSWP. From the reported data, it could be proved that the biosorption of MB dye by DRSWP-biosorbent was not only cost effective but also eco-friendly. In this attempt, the concoction of dried rice husk, sugarcane bagasse and wheat bran powder has been utilized as a biosorbent.

Keywords: Biosorption; Methylene blue; Rice husk; Sugarcane bagasse; Wheat bran; Isotherm studies

1. Introduction

In recent years, the rapid growth of industrialization leads to the release of more contaminants and pollutants to the environment. On the other hand, many Industries use an ample amount of water for the unit operation process causing water scarcity and also discharging the effluent without any prior treatment. Finally, it is drained into the aquatic ecosystem leading to disturbance in the aquatic system. Generally, industries like paper making, printing, dyeing, textiles, food processing, and cosmetics generate colored effluents [1]. These colored effluents from industries, whose concentration is lesser or higher than 1 ppm are more visible and their metabolite causes an inhibitory effect in the aquatic system.

Among the several dyes, methylene blue (MB) has been chosen due to its strong biosorption property onto the solid molecules. MB is a cationic dye molecule that has wide applications in the textile, food, and medical industries. On the contrary, it has several adverse effects on human health and the environment such as shortness in breathing, vomiting, delirium, diarrhea or gastritis, nausea, cause excessive sweating if inhaled through water and also prolonged exposure cause permanent injuries in human and animal eyes [2–4]. Also, artificial or synthetic dyes which are used in food products may cause allergies, hyperactivity

* Corresponding author.

in children, and cancer [5]. To overcome the above issues several methods such as physical, chemical, and biological treatment are used for the decolorization of dye from the effluent. However, physical and chemical methods such as ion-exchange, ozonation [6], nano-membrane filtration [7], photocatalytic degradation [8], coagulation–flocculation [9], electrolysis [10], irradiation [11], conventional adsorption [12] and ultrasonic-assisted adsorption [13] had been extensively studied. And these methods having substantial limitations due to high energy consumption, unable to scale up, and expensive. Above all methods, adsorption was found to be the efficient method due to the following advantages: ease of operation, target specificity, reliability, wide adaptability, cost-effectiveness, and achieving a high level of purification [14–16]. The major limitation in adsorption is adsorbent cost. The most commonly used adsorbent is activated charcoal, which is not viable due to the following drawback: regeneration, expensive, and less available in nature. This results in the search for an alternative adsorbent that can overcome the above drawback.

Many researchers used agroindustry by-products such as rice bran, wheat husk, coconut coir, sawdust, corn straws, pineapple bark, durian husk, hickory wood, banana peels, peanut hull due to its application in the removal of dyes and inexpensive [17–20]. Additionally, India is capable of producing about 117.47 million tonnes of rice, 353.85 million tonnes of sugarcane, and 106.21 million tonnes of wheat, annually [21]. Similarly, due to the high consumption of rice, wheat, and sugarcane, massive amounts of solid wastes such as peel/skin and dregs have been disposed. In the betterment utilization of these wastes, it is suggested to make a low-cost biosorbent to eliminate the dye from aqueous solutions.

Also, these biosorbents (rice husk, sugarcane bagasse, and wheat bran) are highly rich in lignin, cellulose, hemicelluloses, silica, and these materials are highly porous. Cellulose is a common heteropolysaccharide present in the cell wall of these biosorbent, which acts as a sorbent in the dye removing mechanism. Due to the enhanced surface-to-mass ratio, this combined biosorbent aided in the dye removal and was easy to regenerate. Thus the synergistic effect of these three biosorbents has been expected to have higher biosorption capacities. So far, no researchers have reported the MB removal using the combined effect of rice husk, sugarcane bagasse, and wheat bran. Based on the above facts, this is the first report to optimize the synergistic effect of dried rice husk, sugarcane bagasse and wheat bran powder (DRSWP)-biosorbent on MB. The main objectives of the present study are:

- Optimization of equilibrium parameters such as the effect of pH, effect of contact time, effect of initial dye concentration, and effect of biosorbent dosage on percentage removal of MB.
- Determination of biosorption isotherms (Langmuir, Freundlich and Temkin isotherms) and biosorption kinetics.
- Characterization of DRSWP-biosorbent using Fourier-transform infrared spectroscopy (FTIR), scanning electron microscopy (SEM), Brunauer–Emmett–Teller (BET), and X-ray diffraction (XRD) techniques.

2. Materials and methods

2.1. Materials: adsorbate and DRSWP-biosorbent

Methylene blue was procured from Sigma-Aldrich, India. Agricultural wastes such as rice husk, wheat bran, and sugarcane bagasse were obtained from local mills located in Coimbatore and rinsed thoroughly with double distilled water 4–5 times. The stalks of the sugarcane bagasse were cut into small pieces. All the materials were dried under sunlight for 2 d and kept at 80°C for overnight followed by grinding and sieving to obtain a fine powder with a particle size range of 100–125 μm. Powders of three different sources (rice husk, sugarcane bagasse, and wheat bran) were mixed in equal amounts to obtain biosorbent (hereafter DRSWP-biosorbent) and stored in an airtight container until further use. The biosorbent did not experience any physical or chemical treatment before the biosorption experiments.

For equilibrium studies, 100 mL of different concentrations of the dye solution was mixed with 0.5 g of DRSWP-biosorbent and was kept in an orbital shaker for 1 h. The solution was spun in a centrifuge for 15 min at 1,000 rpm and the absorbance of the supernatant was measured at 664 nm using UV-Visible spectrophotometer. The dye removal percentage (% R) and the capacity of biosorbent (Q, mg/g), were determined using the following two equations:

$$\% R = \frac{\left(C_0 - C_e\right)}{C_0} \times 100 \tag{1}$$

$$Q = \frac{\left(C_0 - C_e\right)}{m} \times V \tag{2}$$

where C_0 is the initial dye concentration (ppm) and C_e is the equilibrium dye concentration (ppm), V is the volume of the solution (mL) and m is the mass of the biosorbent (g) [22].

Various equilibrium parameters, with different concentrations of DRSWP-biosorbent were analyzed for the significance of pH, contact time, initial dye concentration and biosorbent dosage. For the evaluation of equilibrium data, various biosorption isothermal studies viz Langmuir, Freundlich, and Temkin isotherms were performed.

2.2. Biosorption kinetics studies

Biosorption of methylene blue by the DRSWP-biosorbent was analyzed using different kinetics equations like pseudo-first-order, pseudo-second-order and intraparticle diffusion models.

2.3. Characterization of DRSWP-biosorbent: FTIR, SEM, BET and XRD

The functional groups in DRSWP-biosorbent before and after biosorption were investigated using the FTIR spectroscopy in the range of 400 to 4,000 cm^{-1}. For sample disc formation, KBr powder was mixed with the dried biosorbent mixture (1:99) and ground into fine powder. By performing the SEM, the external surface region and morphology of the biosorbent (before and after biosorption) were studied. The

surface area and pore volume of the samples were calculated by BET surface analyzer and the structural determination and crystallinity nature of the biosorbent was analyzed using the X-ray diffraction technique

3. Results and discussion

3.1. Equilibrium studies

3.1.1. Effect of pH in the percentage of dye removal and determination of zero point charge (ZPC) of DRSWP-biosobent

From this investigation, the influence of pH of the solution on the biosorption of MB was analyzed by adding 0.50 g of DRSWP-biosorbent in 100 mL of 60 ppm initial dye concentration at different pH values (2–10) and 34°C. 0.1 N NaOH and 0.1 N HCl solutions were used for the adjustment of the pH of the solution. Shaking was fixed for 3 h at a continual speed of 120 rpm. The UV-Vis spectrophotometer was performed for the calculation of the absorbance of dye concentrations at 664 nm. Earlier to the measurements, with the known concentrations of the MB solution, the standard graph was obtained. From Fig. 1, it was understood that the percentage removal of dye was significantly high (>85%) in the basic medium whereas, in an acidic medium, the dye removal capacity was as low as 16.66%. The biosorption of methylene blue dye was the lowest at pH 2 and improved along with the increase in the pH up to 10 with 86% removal of MB. As the solution pH increased, the number of hydroxyl groups in the basic medium also increased, hence, cationic dye methylene blue could easily get biosorbed on the biosorbent surface [23–25]. Hence, it was decided to fix the pH as 10 for further studies.

The charge, biosorption capacity of the biosorbent, and the nature of binding sites were determined using the method zero-point charge. The zero point charge of the biosorbent was done using the solid addition method. In this method, 50 mL of 0.1 M $NaNO_3$ was added to 12 different conical flasks and initial pH (pHi) was adjusted between 1–12 either using 0.1 N HNO_3 or NaOH. After that 0.1 g of DRSWP-biosorbent was added and the suspension was kept in an orbital shaker at 120 rpm for 24 h. The final pH (pHf) was noted after 24 h and ΔpH = pHi – pHf was calculated. The plot of pHi vs. ΔpH shows that (Fig. 2) at pH 7 DRSWP-biosorbent exhibited zero net electrical charges and afterward, the surface of the biosorbent started to gain a negative charge. Hence, due to the electrostatic attraction force, the cationic dye (MB) molecules were bound on the negatively charged biosorbent and the percentage removal of MB was increased in alkaline pH. pH_{ZPC} results also supported the experimental outcome that the optimum pH for MB removal was 10. The high biosorption of MB at alkaline pH was suggested to be due to the presence of OH^- ions that attract cationic dye molecules towards biosorption sites [26–32].

3.1.2. Effect of contact time in percentage of MB removal

To study the impact of biosorption of MB on biosorbent, 0.50 g of DRSWP-biosorbent was added with 100 mL of 60 ppm initial dye concentration and shaken at 120 rpm in an orbital shaker for varied periods (5–60 min) at the optimum pH of 10 to obtain the equilibrium time. Fig. 3 shows a plot of the contact time vs. % removal of methylene blue. Initially, when the adsorbate had contact with the biosorbent, the biosorption rate was as high as 70%, and the reaction attained saturation (equilibrium) at 40 min with 86% removal efficiency. The biosorption rate increased at the beginning of the process because of the availability of high binding sites on the biosorbent surface. After 40 min, due to the unavailability or least binding sites on the surface of the biosorbent, the biosorption rate became almost constant up to 60 min [33]. Hence, it was decided to fix the equilibration time to 40 min for further studies.

3.1.3. Effect of initial MB concentration in percentage of dye removal

In this effect, 0.50 g of DRSWP-biosorbent was blended with 100 mL MB solution of varied concentrations (20, 40, 60, 80 and 100 ppm) and shaken at 120 rpm in an orbital shaker at pH 10 for 40 min. From the graph (Fig. 4), it was explained that the percentage degradation of MB dye was

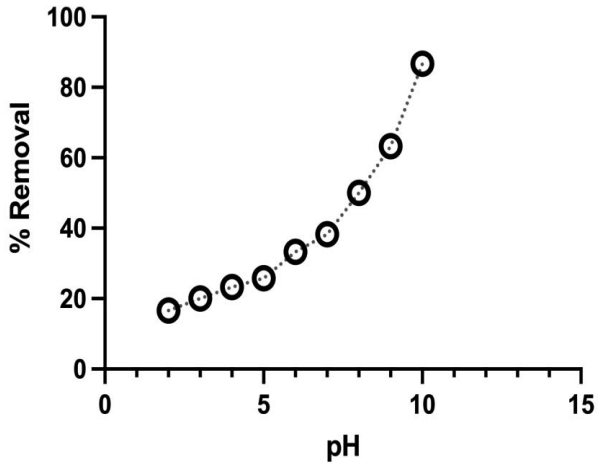

Fig. 1. Effect of pH in percentage of methylene blue removal.

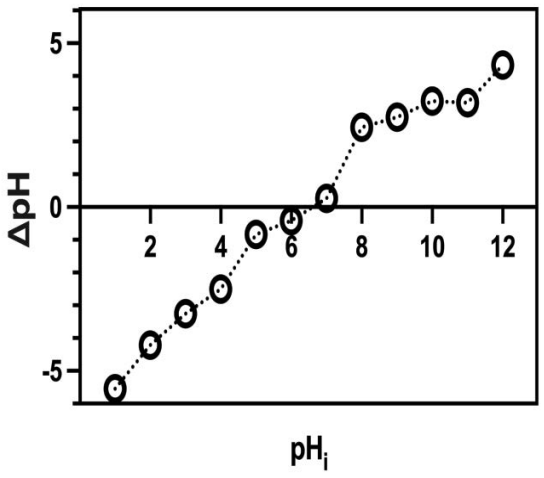

Fig. 2. Zero point charge of DRSWP-biosorbent.

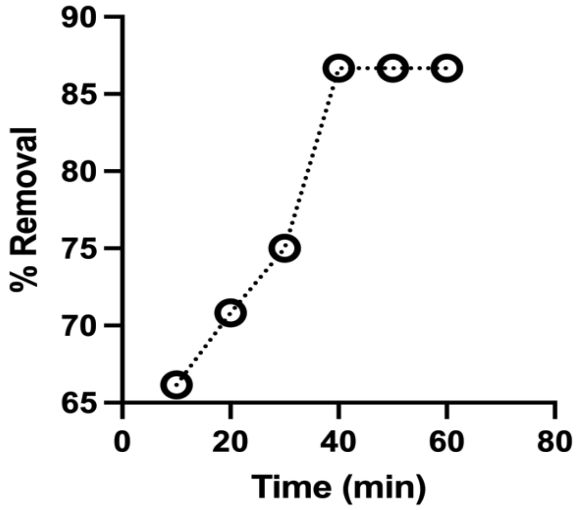

Fig. 3. Effect of contact time in percentage of methylene blue removal.

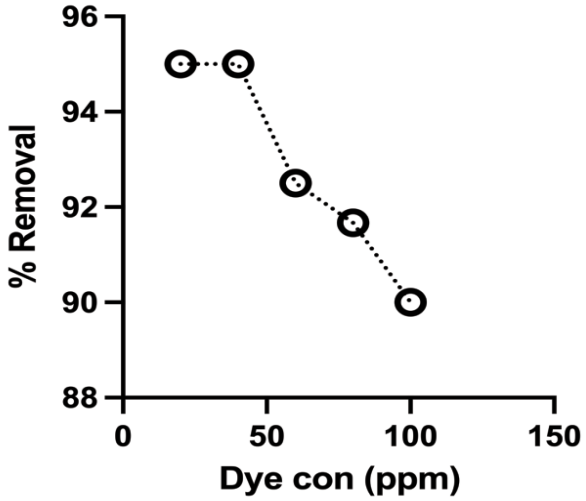

Fig. 4. Effect of initial methylene blue concentration in dye removal percentage.

found as 95% at concentrations of 20 and 40 ppm. The experimental results showed that the percentage elimination of the dye was reduced with the increasing initial concentration of the dye [34].

3.1.4. Effect of biosorbent dosage

The influence of DRSWP-biosorbent dosage on the biosorption of MB was analyzed for different dosages such as 0.2, 0.4, 0.6, 0.8 and 1 g of DRSWP mixed with 100 mL of 40 ppm of the dye solution and agitated at 120 rpm in an orbital shaker at the optimum pH of 10. Increased dosage of DRSWP-biosorbent showed an increased percentage removal as a result of the availability of high binding sites and surface area for the methylene blue adsorbate with the removal percentage ranging from 90%–96% (Fig. 5). Abbas [35] and Olusegun et al. [36] also concluded that the rice husk adsorbent showed a high removal percentage of the methylene blue dye.

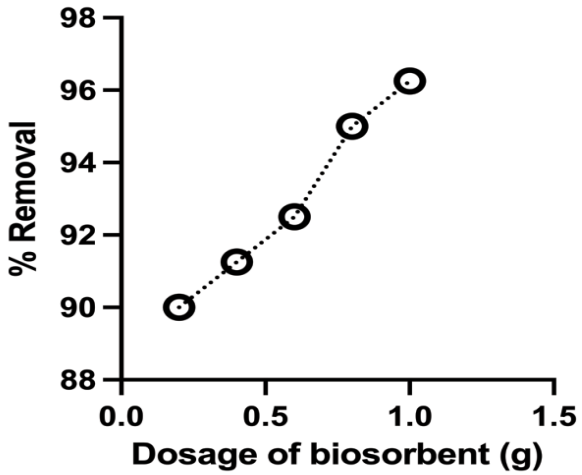

Fig. 5. Effect of biosorbent dosage in percentage of methylene blue removal.

3.2. Biosorption isotherm studies

The isotherm and kinetics of the biosorbent were determined with the working volume of 100 mL containing (the percentage removal was decreased with increasing initial concentration of dyes) [34] various initial MB concentrations (40, 60, 80, 100, 120, and 140 ppm) with 1 g of DRSWP-biosorbent at pH 10. The absorbance of the MB solution was measured at regular intervals at λ_{max} (664 nm) using the UV-Visible spectrophotometer.

3.2.1. Langmuir model

Langmuir isotherm model was used for the determination of biosorption of the dye from the liquid solution. Langmuir model explains the process of biosorption capability of the biosorbents. This model is based on the hypothesis that the process of biosorption happens on a homogeneous surface by forming a monolayer without any contact with the adsorbate molecules. The biosorption process also occurred with an equal adsorbate affinity in all the active sites and the biosorption rate varied in all the biosorption sites.

The Langmuir isotherm equation is represented as follows:

$$q_e = \frac{\left(Q_o b C_e\right)}{\left(1 + b C_e\right)} \tag{3}$$

The Langmuir linear form of equation is:

$$\frac{1}{q_e} = \frac{1}{Q_o b C_e} + \frac{1}{Q_0} \tag{4}$$

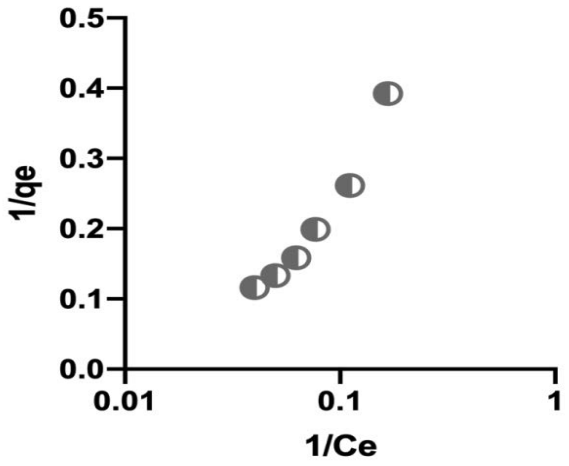

Fig. 6. Langmuir isotherm for methylene blue on DRSWP.

where q_e is the equilibrium biosorption capacity (mg/g) and C_e is the equilibrium concentration of adsorbate (mg/L), Q_o is the monolayer biosorption capacity (mg/g) and b is the Langmuir isotherm constant (L/mg) indicating the affinity of the biosorbent and the adsorbate.

Separation factor (R_L) of Langmuir equation is expressed as follows:

$$R_L = \frac{1}{\left(1 + bC_0\right)} \tag{5}$$

where C_0 denotes the initial MB dye concentration (mg/L). If the R_L value ranges between 0 to 1 it denotes positive biosorption, the R_L value higher than 1 indicates the negative biosorption and R_L value equal to 1 indicates the linear biosorption and if the value of R_L equal to zero then it represents an irreversible biosorption process. The plot of $1/q_e$ vs. $1/C_e$ (Fig. 6) yielded the slope ($1/Q_o b$) and intercept ($1/Q_o$) values. The calculated results were best fitted with the Langmuir isotherm model with the regression coefficient value of 0.999 (Table 1) for MB removal using DRSWP-biosorbent, thereby, explaining the best depiction of biosorption. The maximal monolayer biosorption capacity of DRSWP-biosorbent for the elimination of methylene blue was found to be 39.002 mg/g. For the varied initial concentrations of MB, the separation factor (R_L) was determined, and the values were found in the range of 0.6803–0.3781. All the calculated values of the separation factor were within the range of 0 to 1, thus, showing a positive biosorption of methylene blue onto DRSWP-biosorbent [37–40].

3.2.2. Freundlich isotherm model

This model is used to depict the biosorption characteristics for the heterogeneous surface as well as multilayer biosorption.

Freundlich isotherm is represented by the following equation:

$$q_e = K_F C_e^{1/n} \tag{6}$$

The linearized form of equation is:

$$\log q_e = \log K_F + \frac{1}{n}\log C_e \tag{7}$$

where K_F and n are the Freundlich isotherm constant (mg/g (L/mg)$^{1/n}$) and biosorption intensity, respectively. C_e denotes the equilibrium concentration of the dye (mg/L). q_e denotes the quantity of dye adsorbed per gram of biosorbent (mg/g) at equilibrium. The graph of $\log q_e$ vs. $\log C_e$ (Fig. 7) was used to predict the constants K_F and $1/n$ as presented in Table 1. The favorability of the biosorption process can be indicated based on the value of $1/n$. The $1/n$ value below one represents a favorable biosorption. On the contrary, the value of $1/n$ above one indicates a cooperative biosorption. Freundlich isotherm results showed that the biosorption capacity of non-ideal, heterogeneous biosorption of DRSWP-biosorbent. Since the obtained $1/n$ value was lower than one (0.86041), resulting that MB followed a favorable biosorption. The capacity of the DRSWP-biosorbent and the uptake of dye molecules were explained by the K_F value (0.5609) [37,38,41].

3.2.3. Temkin isotherm model

The relations between the biosorbent and the adsorbate molecules were studied using the Temkin isotherm model. The heat of biosorption that reduced linearly along the surface interactions between adsorbate and the biosorbent in the intermediate adsorbate concentrations.

The Temkin isotherm model is represented in the following linearized form of an equation:

$$q_e = B_T \ln A_T + B_T \ln C_e \tag{8}$$

where $B_T = RT/b$, A_T and b are the equilibrium binding constant (L/g) and Temkin isotherm constant, respectively.

Table 1
Isotherm variables for the biosorption of methylene blue adsorbate upon DRSWP-biosorbent

Langmuir		Freundlich		Temkin	
Q_0 (mg/g)	39.002	K_F (mg/g (L/mg)$^{1/n}$)	0.56087	A_T (L/g)	0.54903
R_L	0.6803–0.3781	$1/n$	0.86041	B_T	4.7152
b (L/mg)	0.0118			b (J/mol)	54.315
R^2	0.99902	R^2	0.99782	R^2	0.9895

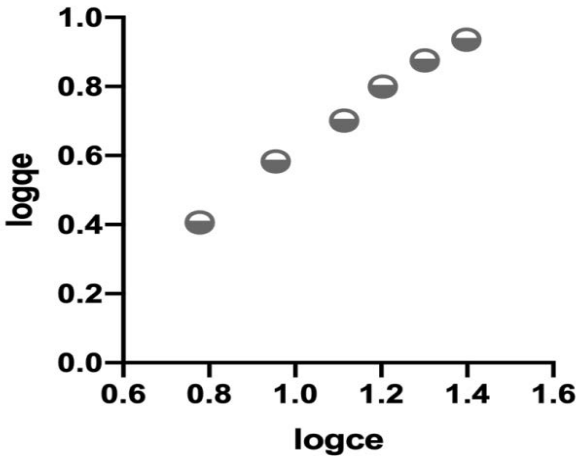

Fig. 7. Freundlich isotherm for methylene blue on DRSWP.

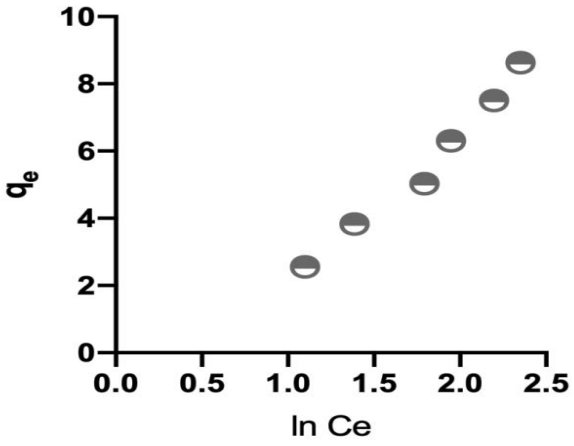

Fig. 8. Temkin isotherm for methylene blue on DRSWP.

R indicates the ideal gas constant (8.314 J/mol K), T denotes the temperature in Kelvin and b is the constant linked to heat of biosorption (J/mol). A graph was plotted as q_e vs. lnC_e (Fig. 8). Constants b and A_T were estimated using the slope and intercept of the graph. Temkin isotherm results showed that the biosorption interactions between the adsorbate and the DRSWP-biosorbent and the maximum binding energy were found as 0.1673 L/g with a high R^2 value as 0.9895. Due to the interactions, the heat of biosorption was decreased linearly with the coverage. The R^2 value of 0.9895 showed that the biosorption also followed the Temkin model [41].

3.3. Biosorption kinetics

The biosorption process of the MB by the DRSWP-biosorbent, controlled by various mechanisms such as chemical reaction, mass transfer and diffusion were determined by the biosorption kinetics model. For the investigation of the controlling mechanisms, the results obtained were investigated by various kinetic models such as pseudo-first-order, pseudo-second-order and intraparticle diffusion models.

3.3.1. Pseudo-first-order kinetic model

This model follows the hypothesis that the capacity of the biosorbent depends upon the rate of change of the dye elimination with respect to time. The equation of pseudo-first-order kinetic is:

$$\log\left(q_e - q_t\right) = \log\left(q_e\right) - \left(\frac{K_1}{2.303}\right)t \tag{9}$$

where q_e is the equilibrium biosorption (mg/g), q_t is the dye biosorption at time t (mg/g), K_1 indicates the pseudo-first-order rate constant (1/min) and t represents time (min).

A linear graph of log(q_e – q_t) vs. time (t) is represented in Fig. 9. The q_e and K_1 values were calculated using linear regression of the plot [42]. Pseudo-first-order kinetics model (Table 2) showed the experimental equilibrium biosorption capacities ($q_{e,\exp}$) as 2.55, 3.825, 5.025, 6.3, 7.5, 8.625 mg/g and the calculated equilibrium biosorption capacities ($q_{e,\text{cal}}$) as 2.85, 4.04, 5.35, 6.63, 7.87, and 8.93 mg/g for the varied concentrations of MB. The $q_{e,\exp}$ values were closer to $q_{e,\text{cal}}$ values attributed that the biosorption is well described by the pseudo-first-order. As the concentration of the dye increased, the biosorption capacities also increased with the increased regression coefficient values. These results concluded that the DRSWP-biosorbent showed a good relationship with the adsorbate MB and also explained that the number of free sites is considerably higher than the number of dye molecules biosorbed [43–47].

Table 2
Pseudo-first and second-order kinetics parameters for the biosorption of methylene blue adsorbate on DRSWP-biosorbent

C_0 (mg/L)	Pseudo-first-order				Pseudo-second-order			
	R^2	K_1 (min^{-1})	$q_{e,\exp}$ (mg/g)	$q_{e,\text{cal}}$ (mg/g)	R^2	K_2 (g/mg min)	H	$q_{e,\text{cal}}$ (mg/g)
40	0.990	0.0089	2.55	2.848	0.991	0.00454	0.00942	–1.44051
60	0.995	0.0053	3.83	4.041	0.9840	0.00359	0.00999	–1.66881
80	0.997	0.0051	5.03	5.348	0.8899	0.00794	0.00969	–1.10528
100	0.990	0.0047	6.30	6.629	0.9427	0.00389	0.013121	–1.8364
120	0.987	0.0036	7.50	7.865	0.9753	0.00813	0.00968	–1.09141
140	0.992	0.0029	8.63	8.933	0.9548	0.00709	0.009898	–1.18152

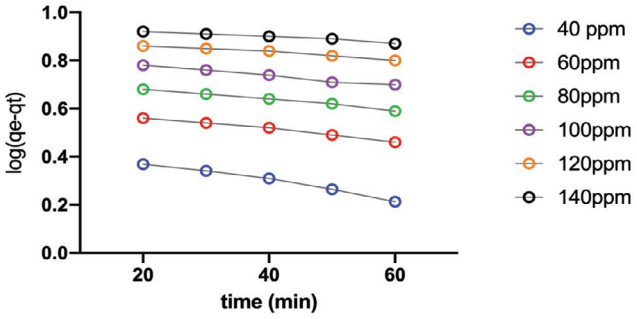

Fig. 9. Pseudo-first-order kinetics of methylene blue on DRSWP.

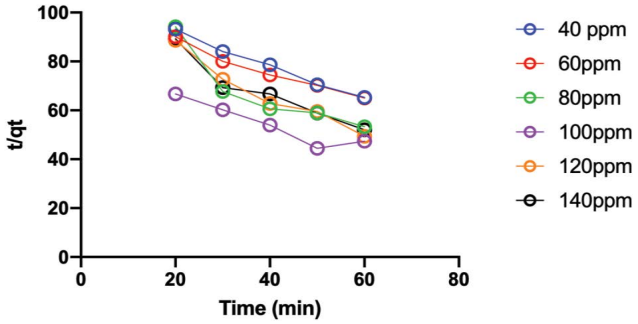

Fig. 10. Pseudo-second-order kinetics of methylene blue on DRSWP.

3.3.2. Pseudo-second-order kinetic model

This model provides the biosorption characteristics throughout the whole period of the biosorption process. This model considers the hypothesis that the biosorption process is related to chemisorption, which occurs between the adsorbate and the biosorbent functional groups with the aid of the energy from electrons. The linearized form of the pseudo-second-order kinetic equation is expressed as follows:

$$\frac{t}{q_t} = \frac{1}{K_2 (q_e)^2} + \left(\frac{1}{q_e}\right) t \tag{10}$$

where K_2 denotes the pseudo-second-order rate constant (g/mg min). q_e and q_t represent the amount of dye biosorbed (mg/g) at equilibrium and at any given time t [42]. The constant values were estimated with the help of the slope and intercept of the plots drawn as t/q_t vs. time (Fig. 10). In the pseudo-second-order kinetics model, the determined biosorption capacities were found to be negative, which represented no significant relation between the adsorbate and the biosorbent. Hence, the pseudo-second-order kinetic model failed to describe the biosorption capacity of DRSWP-biosorbent on MB [44].

3.3.3. Intraparticle diffusion model

The biosorption of dyes upon contact with the biosorbent occur through the following three steps, (i) through molecular diffusion, the adsorbate dye is transferred from the bulk solution to the outer surface of the biosorbent, (ii) localization of biosorbate to the inner surface of the biosorbent and (iii) the biosorption of the adsorbate molecules from the operative sites into the pores of the inner surface of the biosorbent. The intraparticle diffusion model equation is:

$$q_t = K_{in} t^{0.5} + C \tag{11}$$

where K_{in} is the intraparticle diffusion constant (mg/g min$^{0.5}$) and C is the thickness of boundary layer (mg/g). The constant values of the intraparticle diffusion model were determined (Fig. 11) and the values were reported in Table 3. If the biosorption process followed the intraparticle diffusion model, the plot of q_t vs. $t^{0.5}$ would generate an origin passing straight line. The kinetic data were processed to predict whether the intraparticle diffusion was the rate determining step. From Fig. 11 it is evident that there was no straight line passing through the origin and indicated that the non-linearity of the graph. This explained that, intraparticle diffusion was not only the rate limiting step but also revealed that the biosorption process was controlled by other kinetic models such as surface biosorption and intraparticle diffusion. [39,44,48].

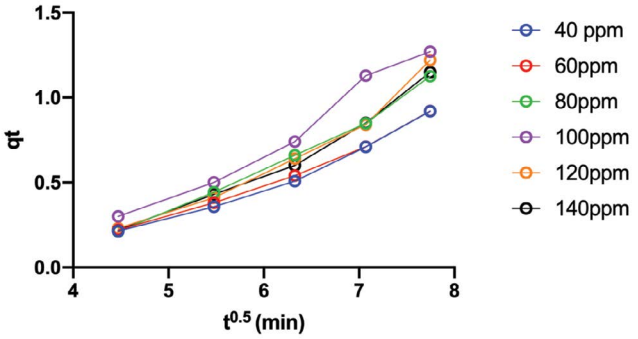

Fig. 11. Intraparticle diffusion of methylene blue on DRSWP.

Table 3
Intraparticle diffusion parameters

C_0 (mg/L)	R^2	K_{in} (mg/g min$^{0.5}$)	C (mg/g)
40	0.986	0.2134	–0.7855
60	0.991	0.2112	–0.7593
80	0.994	0.2717	–1.0321
100	0.986	0.3121	–1.1543
120	0.978	0.2909	–1.1428
140	0.983	0.2752	–1.0595

Table 4 describes the comparison of biosorption capacity of biosorbents with agricultural wastes used for MB removal. The biosorption capacity of DRSWP-biosorbent compared with other biosorbents and found to be 39.007 mg/g which is higher than the biosorption capacities of various low-cost biosorbents and activated carbons for the removal of MB such as rice husk carbon (RHC) [49], rice husk carbon (RHC) [50], sugarcane bagasse activated carbon [51], reticulated formic lignin (RFL) from sugarcane bagasse [52], $CaCl_2$

Table 4
Comparison of biosorption capacities of methylene blue on various agricultural wastes

Biosorbent	Q_m (mg/g)	Reference
Rice husk, sugarcane bagasse, wheat bran (DRSWP)	39.002	Present study
Rice husk carbon (RHC)	28.5	[49]
Rice husk carbon (RHC)	37.57	[50]
Sugarcane bagasse activated carbon	6.73	[51]
Reticulated formic lignin (RFL) from sugarcane bagasse	34.20	[52]
$CaCl_2$ treated sugarcane bagasse (CSGB)	35.2113	[53]
Coir pith carbon prepared from coconut husk	5.87	[54]
Wheat shell (WHS)	21.50	[55]
Wheat straw pre-treated with 1.8 M H_2SO_4	20.41	[56]

treated sugarcane bagasse (CSGB) [53], coir pith carbon prepared from coconut husk [54], wheat shell (WHS) [55], wheat straw pre-treated with 1.8 M H_2SO_4 [56].

3.4. Characterization of biosorbent before and after biosorption: FTIR, SEM, BET and XRD

FTIR analysis (Fig. 12A and B) was performed to explicate the functional group responsible for the removal of MB [57]. Because of the hydrogen bonded OH vibration of the cellulosic structure, FTIR spectrum of DRSWP- biosorbent before biosorption showed stretching at 3,784.90 and 3,288.86 cm^{-1} whereas after biosorption showed multiple stretching vibrations at 3,785.41; 3,696.52; 3,657.60 and 3,278.96 cm^{-1} [58]. The peaks at 2,891.28 cm^{-1} before biosorption and the peaks at 2,886.16 cm^{-1} after biosorption could be attributed to the aliphatic (C–H) alkane groups [59].

In the sample before biosorption, C–O stretching of the carbonyl (C=O) group in hemicellulose was observed at 1,729.96 cm^{-1} before biosorption. However, the carbonyl group after biosorption was observed at 1,727.76 cm^{-1} [58,60]. C–O–C stretching vibrational shift was noticed at 1,061.70 cm^{-1} in samples collected before biosorption, whereas, C–O–C peak in samples collected after biosorption was found at 1,076 cm^{-1} [39]. Before biosorption, the peak was noticed at 898.53 cm^{-1} because of the presence of the C–O–H group. Si–H group could be ascribed to the peaks at 606.56, 562.85, 532.11, 490.79, and 475.32 cm^{-1} before biosorption and 592.96, 533.19, and 463.69 cm^{-1} after biosorption [61].

SEM images of DRSWP-biosorbent before biosorption (Fig. 13A) showed the smooth longitudinal shaped compounds surrounded by small fragments of compounds whereas, after biosorption (Fig. 13B), the morphology of the DRSWP-biosorbent was completely modified into large flake-like structures due to their higher interactions with the adsorbate (Fig. 13) [61].

The surface area and pore volume of the samples were calculated by BET surface analyzer. The BET surface area, saturated vapor pressure, average pore diameter and total pore volume of the biosorbent before and after biosorption were found to be 1.355 m^2/g, 97.99 kPa, 24.726 nm, 8.3795 cm^3/g and 7.538 m^2/g, 98.024 kPa, 7.296 nm, 1.375 cm^3/g respectively. From the reported values, it could be seen that after biosorption the average pore diameter and total pore volume of the biosorbent have been reduced because of the accumulation of MB molecules. From the Fig. 14A and B, it could be seen that a shift (before and after) was occurred due to the biosorption of MB molecules. [23,31].

The structural determination and crystallinity nature of the biosorbent was analyzed using the X-ray diffraction technique. A broad peak was observed (Fig. 15A) at the 2θ 22.145° and another peak at 26.615°. In Fig. 15B, a broad peak was observed at the 2θ 22.32° and another peak at 35.01°. In both figures, the peak was observed for 2θ ranging

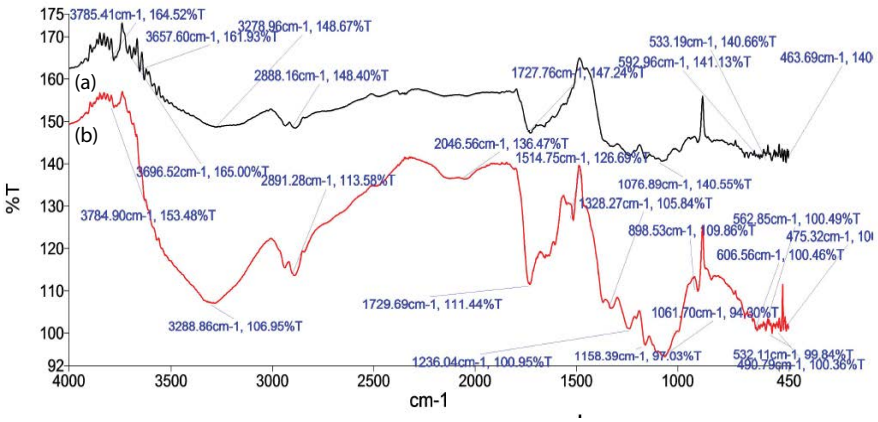

Fig. 12. FTIR spectrum of DRSWP (B) before and (A) after biosorption with methylene blue adsorbate.

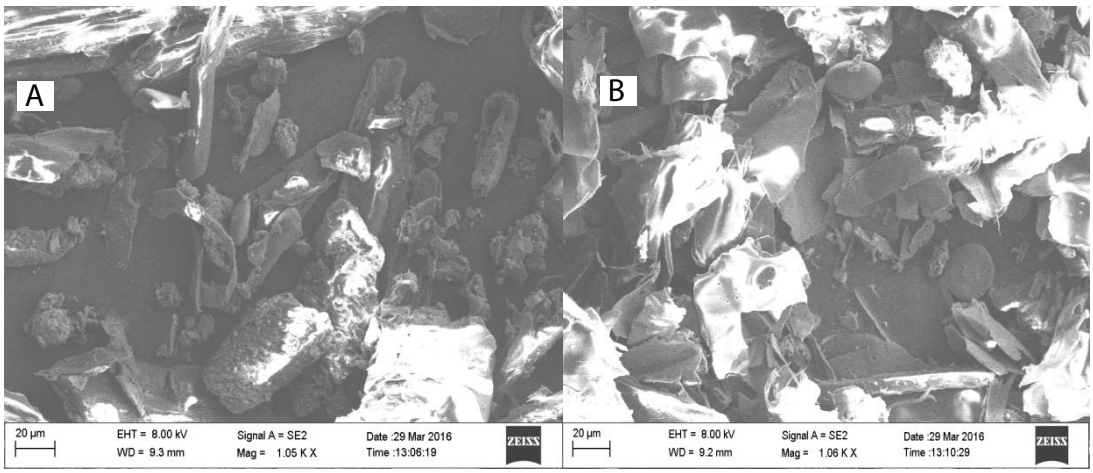

Fig. 13. SEM image of DRSWP (A) before and (B) after biosorption of methylene blue.

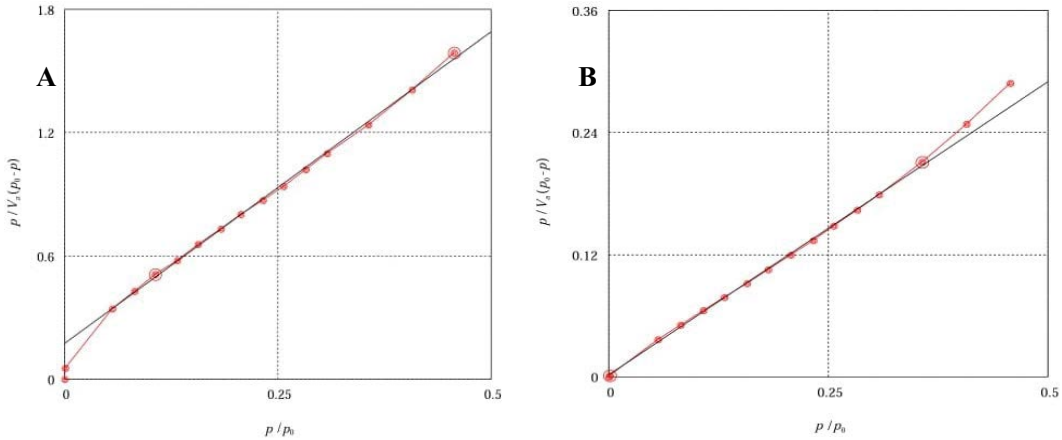

Fig. 14. BET analysis of DRSWP-biosorbent (A) before and (B) after biosorption of methylene blue.

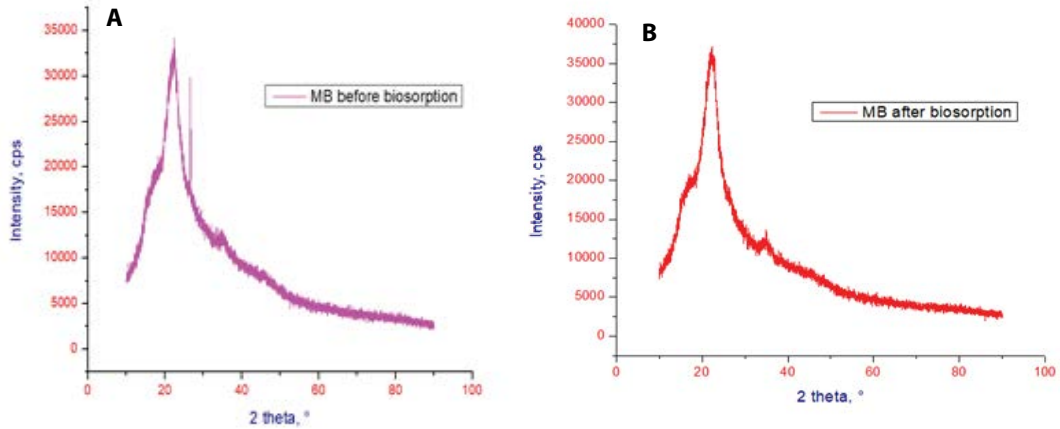

Fig. 15. XRD pattern of DRSWP-biosorbent (A) before and (B) after methylene blue biosorption.

between 22° and 23° and this showed the presence of cellulose I type. Also, the broad peak occurred at 2θ 22.145° (Fig. 15A), and 2θ 22.32° (Fig. 15B) revealed that the amorphous nature of DRSWP-biosorbent. [31,32,62–65].

4. Conclusion

Biomaterials are auspicious biosorbents for the elimination of cationic dyes. The elimination of methylene blue (MB)

from the aqueous solution through DRSWP-biosorbent was analyzed under various experimental conditions in batch mode. The biosorption of dye was dependent on biosorbent dosage, pH, and methylene blue concentration. The optimal values of pH, contact time, initial dye concentration, and biosorbent dosage were estimated as 10, 40 min, 40 mg/L, and 1 g respectively with a removal efficiency of 96%. The equilibrium has been found in the best correlation with the Langmuir isotherm model and revealed that monolayer biosorption occurred. The kinetic study revealed that the pseudo-first-order model fitted well with the experimental values indicating that the biosorption process was dependent upon initial concentrations of MB. The result of the intraparticle diffusion model showed that this model has played an important role in biosorption, and it was not only the rate-limiting step. The present investigation has shown that DRSWP-biosorbent could be effectively used for methylene blue removal. DRSWP-biosorbent is economically cheap, and hence, regeneration is not required.

Acknowledgment

The authors thank the Government College of Technology, Coimbatore, India for providing the work space.

This research did not receive any specific grant from funding agencies in the public, commercial, or not-for-profit sectors.

References

[1] O.S. Bayomi, E.H. Kandeel, T. Shoeib, H. Yang, N. Youssef, M.M.H. El-Sayed, Novel approach for effective removal of methylene blue dye from water using fava bean peels waste, Sci. Rep., 10 (2020) 1–10.
[2] A. Özer, D. Gulbeyi, Removal of methylene blue from aqueous solution by dehydrated wheat bran carbon, J. Hazard. Mater., 146 (2007) 262–269.
[3] Z.M. Lazim, E. Mazuin, T. Hadibarata, Z. Yusop, The removal of methylene blue and remazol brilliant blue r dyes by using orange peel and spent tea leaves, J. Teknol., 74 (2015) 129–135.
[4] S. Soni, P.K. Bajpai, J. Mittal, C. Arora, Utilisation of cobalt doped iron based MOF for enhanced removal and recovery of methylene blue dye from waste water, J. Mol. Liq., 314 (2020) 1–40.
[5] J. Mittal, Permissible synthetic food dyes in India, Resonance, 25 (2020) 567–577.
[6] Y. Liu, X. Zhao, J. Li, D. Ma, R. Han, Characterization of biochar from pyrolysis of wheat straw and its evaluation on methylene blue adsorption, Desal. Water Treat., 46 (2012) 115–123.
[7] H.R. Rashidi, N.M.H. Sulaiman, N.A. Hashim, C.R.C. Hassan, M.R. Ramli, Synthetic reactive dye wastewater treatment by using nano-membrane filtration., Desal. Water Treat., 55 (2015) 86–95.
[8] D. Gümüş, F. Akbal, Photocatalytic degradation of textile dye and wastewater, Water Air Soil Pollut., 216 (2011) 117–124.
[9] C.Y. Teh, P.M. Budiman, K.P.Y. Shak, T.Y. Wu, Recent advancement of coagulation–flocculation and its application in wastewater treatment, Ind. Eng. Chem. Res., 55 (2016) 4363–4389.
[10] R. Lafi, L. Gzara, R.H. Lajimi, A. Hafiane, Treatment of textile wastewater by a hybrid ultrafiltration/electrodialysis process, Chem. Eng. Process., 13 (2018) 105–113.
[11] K. Hossain, Y.A. Maruthi, N.L. Das, K.P. Rawat, K.S.S. Sarma, Irradiation of wastewater with electron beam is a key to sustainable smart/green cities: a review, Appl. Water Sci., 8 (2018) 1–12.
[12] K.Z. Elwakeel, A.M. Elgarahy, S.H. Mohammad, Use of beach bivalve shells located at Port Said coast (Egypt) as a green approach for methylene blue removal, J. Environ. Chem. Eng., 5 (2017) 578–587.
[13] A. Asfaram, M. Ghaedi, S. Hajati, A. Goudarzi, Synthesis of magnetic γ-Fe_2O_3-based nanomaterial for ultrasonic assisted dyes adsorption: modeling and optimization, Ultrason. Sonochem., 32 (2016) 418–431.
[14] I. Anastopoulos, I. Pashalidis, A.G. Orfanos, I.D. Manariotis, T. Tatarchuk, L. Sellaoui, A.B. Petriciolet, A. Mittal, A.N. Delgado, Removal of caffeine, nicotine and amoxicillin from (waste) waters by various adsorbents. A review, J. Environ. Manage., 26 (2020) 1–9.
[15] V.K. Gupta, S. Agarwal, R. Ahmad, A. Mirza, J. Mittal, Sequestration of toxic congo red dye from aqueous solution using eco-friendly guar gum/activated carbon nanocomposite, Int. J. Biol. Macromol., 158 (2020) 1–31.
[16] A. Mariyam, J. Mittal, F. Sakina, R.T. Baker, A.K. Sharma, A. Mittal, Efficient batch and fixed-bed sequestration of a basic dye using a novel variant of ordered mesoporous carbon as adsorbent, Arabian J. Chem., 14 (2021) 1–15.
[17] A.A.H. Saeed, N.Y. Harun, S. Sufian, A.A. Siyal, M. Zulfiqar, M.R. Bilad, A. Vagananthan, A.Al-Fakih, A.A.S. Ghaleb, N. Almahbashi, *Eucheuma cottonii* seaweed-based biochar for adsorption of methylene blue dye, Sustainability, 12 (2020) 1–15.
[18] F.S. Hashem, M.S. Amin, Adsorption of methylene blue by activated carbon derived from various fruit peels, Desal. Water Treat., 57 (2016) 1–12.
[19] M. Sankar, G. Sekaran, S. Sadulla, T Ramas, Removal of diazo and triphenylmethane dyes from aqueous solutions through an adsorption process, J. Chem. Technol. Biotechnol., 344 (1999) 337–344.
[20] V.K. Gupta, R. Jain, S. Varshney, Removal of reactofix Golden Yellow 3 RFN from aqueous solution using wheat husk — an agricultural waste, J. Hazard. Mater., 142 (2007) 443–448.
[21] https://economictimes.indiatimes.com/news/economy/agriculture/indias-2019–20-foodgrain-production-to-hit-a-record-high-of-291-95-million-tonnes-estimates-second-advance-estimate-of-govt/articleshow/74192668.cms
[22] B.H. Hameed, Evaluation of papaya seeds as a novel non-conventional low-cost adsorbent for removal of methylene blue, J. Hazard. Mater., 162 (2009b) 939–944.
[23] R. Saravanakumar, K. Muthukumaran, N. Selvaraju, Enhanced Pb(II) ions removal by using magnetic NiO/biochar composite, Mater. Res. Express, 6 (2019) 1–14.
[24] A. El-Maghraby, H.A. El-Deeb, Removal of a basic dye from aqueous solution by adsorption using rice hulls, Global Nest J., 13 (2011) 90–98.
[25] B. Acemioglu, Batch kinetic study of sorption of methylene blue by perlite, Chem. Eng. J., 106 (2005) 73–81.
[26] A. Zubrik, M. Matik, S. Hredzak, M. Lovas, Z. Dankova, M. Kovacova, J. Briancin, Preparation of chemically activated carbon from waste biomass by single-stage and two-stage pyrolysis, J. Cleaner Prod., 143 (2016) 1–34.
[27] S. Shoukat, H.N. Bhatti, M. Iqbal, S. Noreen, Mango stone biocomposite preparation and application for crystal violet adsorption: a mechanistic study, Microporous Mesoporous Mater., 239 (2017) 180–189.
[28] S. Noreen, H.N. Bhatt, M. Iqbal, F. Hussain, F.M. Sarim, Chitosan, starch, polyaniline and polypyrrole biocomposite with sugarcane bagasse for the efficient removal of Acid Black dye, Int. J. Biol. Macromol., 147 (2020) 439–452.
[29] M. Kerrou, N. Bouslamti, A. Raada, A. Elanssari, D. Mrani, M.S. Slimani, The use of sugarcane bagasse to remove the organic dyes from wastewater, Int. J. Anal. Chem., 2021 (2021) 1–11.
[30] N. Sifoun, A.R. Yeddou, L.H. Nouri, A. Chergui, B. Nadjemi, Kinetic and thermodynamic studies of methylene blue adsorption on sorghum stems, Algerian J. Environ. Sci. Technol., 3 (2020) 1526–1536.
[31] M.K. Uddin, A. Nasar, Walnut shell powder as a low-cost adsorbent for methylene blue dye: isotherm, kinetics, thermodynamic, desorption and response surface methodology examinations, Sci. Rep., 10 (2020) 1–13.

[32] K.N.G. Mtshatsheni, A.E. Ofomaja, E.B. Naidoo, Synthesis and optimization of reaction variables in the preparation of pine-magnetite composite for removal of methylene blue dye, S. Afr. J. Chem. Eng., 29 (2019) 33–41.
[33] V. Vadivelan, K. Vasanth Kumar, Equilibrium, kinetics, mechanism, and process design for the sorption of methylene blue onto rice husk, J. Colloid Interface Sci., 286 (2005) 90–100.
[34] F. Cicek, D. Ozer, A. Ozer, A. Ozer, Low cost removal of reactive dyes using wheat bran, J. Hazard. Mater., 146 (2007) 408–416.
[35] F.S. Abbas, Dyes removal from wastewater using agricultural waste, Adv. Environ. Biol., 7 (2013)1019–1026.
[36] S.J. Olusegun, E.T.F. Freitas, L.R.S. Lara, N.D.S. Mohallem, Synergistic effect of a spinel ferrite on the adsorption capacity of nano bio-silica for the removal of methylene blue, Environ. Technol., 42 (2019) 2163–2176.
[37] A. Basker, P.S.S. Shabudeen, P. Vignesh Kumar, A.P. Shekhar, Sequestration of basic dye from textile industry wastewater using agro-wastes and modeling with ANOVA, Rasayan J. Chem., 7 (2014) 64–74.
[38] H. Lata, V.K. Garg, R.K. Gupta, Removal of a basic dye from aqueous solution by adsorption using *Parthenium hysterophorus*: an agricultural waste, Dyes Pigm., 74 (2007) 653–658.
[39] M. Mathivanan, E.S. Saranathan, Sugarcane bagasse-a low cost adsorbent for removal of methylene blue dye from aqueous solution, J. Chem. Pharm. Res., 7 (2016) 817–822.
[40] S. Rangabhashiyam, S. Lata, P. Balasubramanian, Biosorption characteristics of methylene blue and malachite green from simulated wastewater onto *Carica papaya* wood biosorbent, Surf. Interfaces, 10 (2018) 197–215.
[41] A.O. Dada, A.P. Olalekan, A.M. Olatunya, O. Dada, Langmuir, Freundlich, Temkin and Dubinin – Radushkevich isotherms studies of equilibrium sorption of Zn^{2+} unto phosphoric acid modified rice husk, J. Appl. Chem., 3 (2012) 38–45.
[42] B.H. Hameed, A.A Ahmad, Batch adsorption of methylene blue from aqueous solution by garlic peel, an agricultural waste biomass, J. Hazard. Mater., 164 (2009a) 870–875.
[43] S.S. Imam, M. Abdullahi, Adsorptive removal of methylene blue using groundnut shell activated carbon coated with Fe_2O_3, J. Appl. Chem., 10 (2017) 12–21.
[44] E.K. Conrad, O.J. Nnaemeka, A.O. Chris, Adsorptive removal of methylene blue from aqueous solution using agricultural waste: equilibrium, kinetic and thermodynamic studies, Am. J. Mater. Sci., 2 (2015) 14–25.
[45] B.H. Hameed, M.I. El-Khaiary, Sorption kinetics and isotherm studies of a cationic dye using agricultural waste: broad bean peels, J. Hazard. Mater., 154 (2008) 639–648.
[46] K.C. Bedin, A.C. Martins, A.L. Cazetta, O. Pezoti, V.C. Almeida, KOH-activated carbon prepared from sucrose spherical carbon: adsorption equilibrium, kinetic and thermodynamic studies for methylene blue removal, Chem. Eng. J., 286 (2016) 476–484.
[47] C. Sabarinathan, P. Karuppasamy, C.T. Vijayakumar, T. Arumuganatha, Development of methylene blue removal methodology by adsorption using molecular polyoxometalate: kinetics, thermodynamics and mechanistic study, Microchem. J., 146 (2019) 315–326.
[48] F. Deniz, S.D. Saygideger, Equilibrium, kinetic and thermodynamic studies of Acid Orange 52 dye biosorption by *Paulownia tomentosa* Steud. leaf powder as a low-cost natural biosorbent, Bioresour. Technol., 101 (2010) 5137–5143.
[49] P.M.K. Reddy, K. Krushnamurty, S.K. Mahammadunnisa, A. Dayamani, Ch. Subrahmanyam, Preparation of activated carbons from bio-waste: effect of surface functional groups on methylene blue adsorption, Int. J. Environ. Sci. Technol., 12 (2015) 1363–1372.
[50] K. Nagarethinam, M.M. Sundaram, Kinetics and mechanism of removal of methylene blue by adsorption on various carbons—a comparative study, Dyes Pigm., 51 (2001) 25–40.
[51] R. Hazzaa, M. Hussein, Cationic dye removal by sugarcane bagasse activated carbon from aqueous solution, Global Nest J., 17 (2015) 1–12.
[52] N.C. Filhoa, E.C. Venancioa, M.F. Barriquelloa, A.A.W. Hechenleitnerb, E.A.G. Pinedab, Methylene blue adsorption onto modified lignin from sugarcane bagasse, Eclética Química J., 32 (2008) 63–70.
[53] H.D. Utomo, R.Y. Natalie Phoon, Z. Shen, L.H. Ng, Z.B. Lim, Removal of methylene blue using chemically modified sugarcane bagasse, Nat. Resour., 6 (2015) 209–220.
[54] D. Kavitha, C. Namasivayam, Experimental and kinetic studies on methylene blue adsorption by coir pith carbon, Bioresour. Technol., 98 (2007) 14–21.
[55] Y. Bulut, H. Aydın, A kinetics and thermodynamics study of methylene blue adsorption on wheat shells, Desalination, 194 (2006) 259–267.
[56] F. Batzias, D. Sidiras, E. Schroeder, C. Weber, Simulation of dye adsorption on hydrolyzed wheat straw in batch and fixed-bed systems, Chem. Eng. J., 148 (2009) 459–472.
[57] S. Sadaf, H.N. Bhatti, S. Ali, K. Rehman, Removal of Indosol Turquoise FBL Dye from aqueous solution by bagasse, a low-cost agricultural waste: batch and column study, Desal. Water Treat., 52 (2013) 37–41.
[58] C. Weng, Y. Lin, T. Tzeng, Removal of methylene blue from aqueous solution by adsorption onto pineapple leaf powder, J. Hazard. Mater., 170 (2009) 417–424.
[59] M. Uddin, M. Islam, S. Mahmud, M. Rukanuzzaman, Adsorptive removal of methylene blue by tea waste, J. Hazard. Mater., 164 (2009) 53–60.
[60] S. Wang, P. Li, J. Gu, H. Liang, J. Wu, Carboxylate-functionalized sugarcane bagasse as an effective and renewable adsorbent to remove methylene blue, Water Sci. Technol., 2017 (2018) 1–10.
[61] P. Sharma, R. Kaur, C. Baskar, W. Chung, Removal of methylene blue from aqueous waste using rice husk and rice husk ash, Desalination., 259 (2010) 249–257.
[62] D.R. Mulinari, H.J.C. Voorwald, M.O.H. Cioffi, G.J. Rocha, M.C.P. Silva, Surface modification of sugarcane bagasse cellulose and its effect on mechanical and water absorption properties of sugarcane bagasse cellulose/HDPE composites, Bioresources, 5 (2010) 661–671.
[63] W. Yang, Y. Feng, H. He, Z. Yang, Environmentally-friendly extraction of cellulose nanofibers from steam-explosion pretreated sugar beet pulp, Materials, 11 (2018) 1–11.
[64] I. Besbes, S. Alila, S Boufi, Nanofibrillated cellulose from TEMPO-oxidized eucalyptus fibres: effect of the carboxyl content, Carbohydr. Polym., 84 (2011) 975–983.
[65] F.S. Nworie, F.I. Nwabue, W. Oti, E. Mbam, B.U. Nwali, Removal of methylene blue from aqueous solution using activated rice husk biochar: adsorption isotherms, kinetics and error analysis, J. Chil. Chem. Soc., 64 (2019) 4365–4376.